

Serveur Académique Lausannois SERVAL serval.unil.ch

Author Manuscript

Faculty of Biology and Medicine Publication

This paper has been peer-reviewed but does not include the final publisher proof-corrections or journal pagination.

Published in final edited form as:

Title: Method validation of nanoparticle tracking analysis to measure pulmonary nanoparticle content: the size distribution in exhaled breath condensate depends on occupational exposure.

Authors: Sauvain JJ, Suarez G, Edmé JL, Bezerra OM, Silveira KG, Amaral LS, Carneiro AP, Chérot-Kornobis N, Sobaszek A, Hulo S

Journal: Journal of Breath Research

Year: 2017 Jan 24

Issue: 11

Volume: 1

Pages: 016010

DOI: [10.1088/1752-7163/aa56dd](https://doi.org/10.1088/1752-7163/aa56dd)

In the absence of a copyright statement, users should assume that standard copyright protection applies, unless the article contains an explicit statement to the contrary. In case of doubt, contact the journal publisher to verify the copyright status of an article.

Method validation of nanoparticle tracking analysis to measure pulmonary nanoparticle content: the size distribution in exhaled breath condensate depends on occupational exposure.

Sauvain J.-J.¹, Suarez G.¹, Edmé J.-L.², Bezerra O.M.P.A.³, Silveira K.G.³, Amaral L.S.⁴, Carneiro A.P.⁵, Chérot-Kornobis N.², Sobaszek A.², Hulo S.²

¹: Institute for Work and Health, University of Lausanne and Geneva, Epalinges-Lausanne, Switzerland

²: University of Lille, CHU Lille, EA 4483 - IMPECS – IMPact de l'Environnement Chimique sur la Santé Humaine, F-59000 Lille, France

³: School of Medicine, Federal University of Ouro Preto, Ouro Preto, Minas Gerais, Brazil.

⁴: FUNDACENTRO, São Paulo, Brazil

⁵: Federal University of Minas Gerais, Belo Horizonte, Brazil

Jean-Jacques Sauvain, Institute for Work and Health, Route de la Corniche 2, 1011 Epalinges, Switzerland. Tel: +41 21 314 74 34; Fax: +41 21 314 74 20
email: jean-jacques.sauvain@hospvd.ch

Guillaume Suarez, Institute for Work and Health, Route de la Corniche 2, 1011 Epalinges, Switzerland. Tel: +41 21 314 58 97; Fax: +41 21 314 74 20
email: guillaume.suarez@chuv.ch

Jean-Louis Edmé, Université de Lille (EA 4483) – Pôle Recherche – 2^{ème} étage aile EST, 1, place Verdun, 59000 Lille, France. Tel: +33 320 626 897; Fax: +33 320 627 784
email: jean-louis.edme@univ-lille2.fr

Olivia Maria de Paula Alves Bezerra, School of Medicine, Federal University of Ouro Preto, Ouro Preto, MG, 35400-000, Brazil. Tel: +55 31 3559-1009; Fax: +55 31 3559-1001
email: ompab@yahoo.com.br

Keller Guimarães Silveira, Medicine School, Federal University of Ouro Preto, Ouro Preto, MG, 35400-000, Brazil. Tel: +55 31 3559-1009; Fax: +55 31 3559-1001
email: kellergs1@hotmail.com

Lenio Sérgio Amaral, FUNDACENTRO, Rua Capote Valente, Nº 710, São Paulo, Brazil. Tel: +55 31 3273-3766; Fax: +55 31 3273-5313
email: lenio.amaral@fundacentro.gov.br

Ana Paula Scalia Carneiro, State Workers' Health Service, Hospital das Clinicas, Federal University of Minas Gerais, Belo Horizonte, Brazil. Tel: +55 31 3273-3911; email: anapaula.scalia@gmail.com

Nathalie Chérot-Kornobis, Université de Lille (EA 4483) – Pôle Recherche – 2^{ème} étage aile EST, 1, place Verdun, 59000 Lille, France. Tel: +33 320 627 762; Fax: +33 320 627 784
email: nathalie.cherot@univ-lille2.fr

Annie Sobaszek, Université de Lille (EA 4483) – Pôle Recherche – 2^{ème} étage aile EST, 1, place Verdun, 59000 Lille, France. Tel: +33 320 623 490; Fax: +33 320 627 784
email: annie.sobaszek@chru-lille.fr

Sébastien Hulo, Université de Lille (EA 4483) – Pôle Recherche – 2^{ème} étage aile EST, 1, place Verdun, 59000 Lille, France. Tel: +33 320 627 761; Fax: +33 320 627 784
email: sebastien.hulo@univ-lille2.fr

Corresponding author:

Jean-Jacques Sauvain, Institute for Work and Health, Route de la Corniche 2, 1011 Epalinges, Switzerland. Tel: +41 21 314 74 34; Fax: +41 21 314 74 20
email: jean-jacques.sauvain@hospv.ch.ch

Total words:

Text/figures: 5,073

Tables: 640

Total : 5,713

Method validation of nanoparticle tracking analysis to measure pulmonary nanoparticle content: the size distribution in exhaled breath condensate depends on occupational exposure.

Abstract

A particle exposure assessment based on the dose deposited in the lungs would be the gold standard for the evaluation of any resulting health effects. Measuring particles in exhaled breath condensate (EBC)—a matrix containing water and airway lining fluid—could help to evaluate particle retention in the lungs.

This study aimed to (1) validate a nanoparticle tracking analysis (NTA) method for determining the particle number concentration and their hydrodynamic size distribution in EBC, and (2) apply this method to EBC collected from workers exposed to soapstone (n = 55) or quartz dust (n = 12) and controls (n = 11).

A standard latex bead solution was used to determine the linear range, limit of detection (LOD), repeatability (coefficient of variation, CV), and bias in spiked EBC. An LM10 NanoSight instrument with NTA version 3.1 software was used for measurement. RTubes® were used for field collection of EBC.

The repeatability obtained for a D_{50} size distribution in EBC showed less than 8% variability, with a bias < 7%. The particle concentration was linear in the range $\leq 2.5 \times 10^8$ particles ml^{-1} with a LOD of 4×10^6 particles ml^{-1} . A recovery of $117 \pm 20\%$ at 6.2×10^7 particles ml^{-1} was obtained with a CV < 10% and a bias < 20%. EBC from workers exposed to quartz, who experienced the largest exposure to silica particles, consistently exhibited a statistically significant ($p < 0.01$) higher concentration of particles in their EBC, with a size distribution shift towards larger values than the other groups. Results showed that the NTA technique performed well for characterizing the size distribution and concentrations of particles in EBC. The technique needs to be corroborated with a larger population of workers.

Keywords:

Exhaled breath condensate; nanoparticle tracking analysis; biological exposure indices; soapstone; quartz

Introduction

One toxicologically important method for evaluating an exposure which could drive the onset of a biological effect is the measurement of the retained dose of particles in the lungs [1]. The retained dose corresponds to the difference between the deposited dose and the amount of particles cleared from the organ. The combination of these two measurements gives the retained dose, which is a function of the deposition site and the interactions between particles and the cellular constituents of the inner lung surface [2]. A retention half-time of up to 700 days has been reported for microparticles deposited in the alveoli [3]. Determining this retained dose in real-life situations is challenging because information about the factors affecting lung deposition (physicochemical properties of the particles, lung morphology, and respiratory conditions) and clearance (dissolution, metabolization, or elimination/translocation) are seldom available [4, 5]. That is why exposure is always evaluated experimentally by determining the amount of particles (mass or number) in the air. Ultrafine particles (particles < 100 nm) are recognized as toxicologically important constituents of aerosols, and they generally dominate number-based particulate size distributions. They thus contribute significantly to the retained dose in the lungs (expressed as a particulate number concentration) due to their decreased clearance [2] and low translocation rate across the epithelial–endothelial barrier [4]. Thus, in the context of an evaluation of the health effects induced by particulate exposure [6], it would seem important to focus on the fine–ultrafine fraction of the particles retained in the lung.

By cooling a subject's exhaled breath in a non-invasive way, it is possible to collect a liquid composed mainly of water and a very small amount of airway lining fluids (ALF) [7]. This technique is thought to allow the collection of ALF from the central region of the lung, as well as from peripheral regions. Due to its simplicity and non-invasiveness, exhaled breath condensate (EBC) is an appealing tool with which to diagnose or assess lung inflammation. Nevertheless, some of the major challenges to be solved before this technique can be routinely applied in clinical settings are the standardization of EBC collection, validation of the analytical techniques used to quantify selected biomarkers, and the determination of reference values [7-8]. Very few studies have reported measuring particulate concentrations in EBC as a tool for exposure assessment in occupational or environmental situations [9-15]. However, the methods used were either qualitative [9, 15] or the relevant statistics in the quantitative ones were either unavailable [10, 12-14] or incomplete [11]. Thus, confidence in the obtained data is low. In

addition to spectroscopic methods, other non-destructive techniques, like dynamic light scattering (DLS) or nanoparticle tracking analysis (NTA), are available for measuring particle concentrations in suspension and their corresponding hydrodynamic size distributions. The significant advantages of NTA, compared to other DLS systems, are its high sensitivity and its ability to characterize each particle present in the liquid, thus allowing accurate sizing of polydisperse samples [16]. The NTA technique has also been standardized by ASTM International (ASTM E2834-12) and is under review at the International Organization for Standardization (ISO/DIS 19430) [17]. This technique was recently applied to determine the particle concentrations in the EBC of non-smokers exposed to second-hand cigarette smoke [12] and for evaluating the ultrafine particle concentrations in the EBC of asthmatic children [13].

The present study's aims were (1) to validate an NTA method for determining the particle number concentration and hydrodynamic size distribution in EBC by evaluating the linear range and limit of detection/quantification for concentration measurement, in addition to evaluating repeatability and bias, and (2) to apply this method to the EBC collected from two different groups of exposed workers, as well as to controls.

Materials and methods

NTA and software

In order to visualize nanoparticles in aqueous solutions, a laser beam is passed through a cell containing the particle suspension. All the particles present in the laser beam will scatter light, allowing their Brownian motion to be recorded via a camera mounted on a microscope. The resulting video is treated frame-by-frame to determine the average distance moved by each particle identified. This information allows us to determine a hydrodynamic size based on the Stokes-Einstein equation [17]. As the field of view is fixed, the sample's scattering volume is known and concentration can be determined based on the number of identified scattering particles. Additionally, the light intensity reaching each pixel in the camera can also be recorded and averaged for each particle. The NTA system used consisted of an LM10 platform (Malvern Instruments, Malvern, UK), including a temperature control, with an sCMOS camera using a 532 nm wavelength laser. The latest NTA version 3.1 software was used, which allows size distribution and concentration to be measured more accurately, as demonstrated by different round robin tests [17]. Approximately 0.4 ml of the sample was injected into the cell using a 1 ml plastic disposable syringe (BD Luer-Lok, Franklin Lakes, USA). Five separate 60-second videos

of each sample were carefully recorded in scatter mode while ensuring the same camera position under the microscope and identical camera settings. After each sample, the cell was cleaned with deionized water and dried with compressed air. After processing using the NTA software, the variables of interest (mean particle size, mode particle size, concentration, and particle size with cumulative percentages smaller than 10%, 50% or 90%, i.e. D_{10} , D_{50} , D_{90}) were averaged from the resulting output summary data file.

Validation

The validation process was carried out using a suspension of concentrated polystyrene latex (PSL) beads (Malvern Instruments, Malvern, UK) with a nominal size of 100 nm and an experimental concentration of $(1.68 \pm 0.04) \cdot 10^{11}$ particles ml^{-1} . This concentration was determined by using a PSL “reference” suspension whose concentration, $(3.42 \pm 0.29) \cdot 10^8$ particles. ml^{-1} , was determined during a Q-Nano round robin test. The Milli-Q[®] water used for the dilution was systematically filtered through a 0.02 μm Anotop 25 filter (Whatman GmbH, Germany), avoiding glass containers. RTubes[®] (Respiratory Research Inc., Austin, USA) were used to collect EBC from each volunteer over different days, as described below. Totals of about 10 ml were pooled, aliquoted in microtubes (Sarstedt, Nümbrecht, Germany), and stored at -20°C until used for exactitude/bias determination.

The method’s performance was determined using the NFT 90-210 protocol [18]. The concentration linearity was evaluated in a rather low range, as EBC is a quite dilute matrix. Eight PSL standards in Milli-Q[®] water ($0\text{--}2.6 \cdot 10^8$ particles ml^{-1}) were prepared each day on four different days and measured using NTA. The limit of quantification (LOQ) was determined using an *a priori* estimation and verifying that its accuracy was smaller than an acceptable maximal deviation from the LOQ, set at 60%. The limit of detection (LOD) then corresponds to one third of the LOQ. The method’s accuracy and bias were evaluated by spiking the pooled EBC with two different concentrations ($1.2 \cdot 10^7$ and $2.4 \cdot 10^7$ particles ml^{-1}) of the PSL stock solution. These suspensions were analyzed without further treatment. A minimum of four independent measurements were done in intermediate precision conditions. Finally, we verified that the different RTubes[®] and microtubes used contained no particles by adding 2 ml and 0.6 ml of filtered water to each consumable, respectively, and shaking/vortexing for at least 2 minutes. On average, fewer than one particle frame^{-1} could be detected—well below the LOD. We also made a preliminary evaluation of the between-day variability in the particle concentrations and size

distributions by measuring these parameters in EBC collected at different times on three consecutive days for one non-smoking volunteer.

Field study

Population

We conducted an exposed-control study on a population of 12 crystal quartz stone workers exposed to quartz dust, 55 soapstone workers exposed to steatite dust, and 11 unexposed control subjects, all recruited between May and October 2014.

The crystal quartz stone workers work in Corinto (Minas Gerais, Brazil), in partially open work sheds, producing decorative crystal objects. The production process consists of cutting, faceting, grinding, and polishing crystal quartz stones with the aid of motorized equipment and grinding or buffing wheels. For polishing, silicon carbide dust or tripoli (silica flour) are used as loose abrasives. Workers shared a common environment and most individuals performed more than one task.

The soapstone workers work in rural areas of Ouro Preto (Mata Dos Palmitos and Santa Rita) or Mariana (Cachoeira do Brumado, Minas Gerais, Brazil), also in partially open work sheds, producing ornamental objects and cooking tools like pans or plates. They grind and shape soapstone blocks using motorized equipment, like grinding wheels or lathes. Workers also shared a common environment and most of them performed more than one task.

Controls were recruited at the University of Ouro Preto. All controls who had been exposed to quartz or soapstone dust were excluded.

All the subjects were fully informed about the study's aims and gave their prior, free, and informed consent. The study was approved by the Ethics Committees on Research at the Federal University of Minas Gerais (Report 183/08) and the Federal University of Ouro Preto (reference 0063.0.238.000-10).

Exposure Assessment

Personal respirable dust samples were taken using a pump (Buck VSS 05, A. P. Buck Inc, Orlando, FL) connected to cyclones with PVC membrane filters, using a constant flow of 1.7 L min⁻¹ ± 5%. The concentration of the respirable particles in the air was obtained using certified gravimetric methods [19]. The silica content of the respirable dust was determined by

sequentially calcinating the filters, re-suspending the residue, and depositing it on PVC-acrylonitrile filters for X-ray diffractometry (X'Pert-Pro, Panalytical) [20]. For crystal quartz stone workers, 52 personal respirable dust samples, covering all tasks, were collected in six work sheds between March and May 2014. For soapstone workers, 32 personal respirable dust personal samples, covering all tasks, were collected in nine work sheds in October 2014.

EBC collection

The EBC samples were collected on a single workday at a clean location away from the exposed subjects' workplaces, i.e. at the Health Examination Centre in Corinto, for the crystal quartz stone workers, and at the Federal University of Ouro Preto, for the soapstone workers and the controls. The EBC samples were collected over 15 minutes using RTubes[®] (Respiratory Research Inc., Charlottesville, VA, USA) and nose clips, according to the latest recommendations [21]. We took care to avoid contamination and isolate the EBC samples by sealing the used polypropylene tubes with caps, immediately after collection and without further treatment. EBC samples were transported at -20°C and stored at -80°C until analysis. All the EBC samples were divided into aliquots in the same room at the end of the subject enrolment period.

After thawing and vortexing, EBC sample was aspirated using a 1 ml plastic syringe and injected into the LM10 module, taking care to avoid bubbles. The solution was measured without any further treatment.

Some EBC samples were also observed using a scanning electron microscope (SEM). Five samples of 3 μl of each EBC were sequentially added and evaporated on a carbon-coated SEM grid (Formav, Plano, Wetzlar, Germany), under a laminar hood, in order to avoid contamination from ambient particles. A SEM (Phenom XL, Phenom-World BV, Eindhoven, The Netherlands) incorporating an energy dispersing X-ray spectrometer allowing elemental analysis was used to characterize the particles observed.

Spirometric measurements

After EBC collection, all subjects were instructed to performed forced expiratory maneuvers (for at least 6 seconds) using the COPD-6 device (Model 4000, Vitalograph, Ennis, Ireland). Data were expressed as ratios of observed/predicted values using reference values for Brazilian adults [22].

Data analysis

Statistical analyses were performed using SAS (SAS Institute Inc., Cary, NC, USA, version 9.3) and STATA 13 software (StataCorp LP, College Station, TX, USA).

Values were expressed as mean and standard deviation or median with interquartile range. Repeatability was assessed using CV. Analysis of variance (one-way ANOVA) was used to test for average differences between groups, and post hoc comparisons were determined with a Bonferroni correction. Correlations between two quantitative variables were determined with the Pearson correlation. Analysis of contingency tables was performed using the chi-squared test.

Results

Validation

Size measurement

The NTA technique was initially developed for precise size determination. Table 1 indicates its very good repeatability for standard solutions of PSL beads (< 5%).

Table 1: Summary of NTA's performance in the determination of the particle size distribution in a standard solution (latex beads-PSL) and EBC.

Method characteristics	Expected performance	Observed value	Conclusion
<i>Repeatability</i>			
Mode; PSL standard $1.2 \cdot 10^7 \text{ \# ml}^{-1a}$	100 nm	$106 \pm 5 \text{ nm}$	Verified
CV ^b mode	5%	4.5%	Verified
D ₅₀ ; PSL standard $1.2 \cdot 10^7 \text{ \# ml}^{-1}$	100 nm	$101 \pm 5 \text{ nm}$	Verified
CV D ₅₀	5%	4.6%	Verified
Mode; EBC not spiked	-	$118 \pm 13 \text{ nm}$	
CV mode	-	11%	
D ₅₀ ; EBC not spiked	-	$137 \pm 10 \text{ nm}$	
CV D ₅₀	-	8%	
<i>Accuracy</i>			
Reference value D ₅₀ ; EBC spiked $1.2 \cdot 10^7 \text{ \# ml}^{-1}$	100 nm	$104 \pm 6 \text{ nm}$	
CV		5.9%	
Maximum accepted range	$\pm 20 \text{ nm} = 20\% \cdot 100 \text{ nm}$		
Upper accepted value	120 nm	116 nm	Verified
Lower accepted value	80 nm	92 nm	Verified
Reference value D ₅₀ ; EBC spiked $2.4 \cdot 10^7 \text{ \# ml}^{-1}$	100 nm	$106 \pm 7 \text{ nm}$	
CV		6.5%	
Maximum accepted range	$\pm 20 \text{ nm} = 20\% \cdot 100 \text{ nm}$		
Upper accepted value	120 nm	119 nm	Verified
Lower accepted value	80 nm	92 nm	Verified

^a: \# ml^{-1} : particles ml^{-1}

^b: CV: coefficient of variation

For biological samples like EBC, we observed that the mode value presented a larger variability (11%) than the D₅₀ measurement (8%). As no EBC reference material is available, we spiked

EBC at ~50% and 100% of the initially measured particle concentration. The measured D_{50} size of spiked EBC at $1.2 \cdot 10^7$ and $2.4 \cdot 10^7$ particles ml^{-1} (104 ± 6 nm and 106 ± 7 nm, respectively) corresponded well to the measured size of the PSL beads (101 ± 5 nm). The accuracy of the D_{50} size measurement in EBC was within 20% of the reference value and can be considered as quite good.

Concentration measurement

Table 2 presents the important figures from the particle concentration measurements using the NTA technique. The calibration range was observed to be linear, at least up to $2.6 \cdot 10^8$ particles ml^{-1} (see Figure S1, Supplemental material). Based on this calibration curve, we postulated an LOQ at $1.3 \cdot 10^7$ particles ml^{-1} . The bias observed at this concentration was indeed smaller than 60% of the LOQ, as proposed by the NFT 90-210 standard. An LOD of $4.3 \cdot 10^6$ particles ml^{-1} was then calculated based on this LOQ. The average particle concentration of non-spiked EBC was $2.94 \pm 0.62 \cdot 10^7$ particles ml^{-1} ($n = 5$). The repeatability (CV) was greatest (21% variability) for the non-spiked EBC and decreased to about 10% for spiked samples at levels around $4\text{--}6 \cdot 10^7$ particles ml^{-1} . A very good recovery rate, comprised between $100\text{--}117 \pm 20\%$ was determined for spiked EBC samples with PSL beads. As a reference solution with a known PSL concentration was available from a Q-Nano round robin test, the accuracy of the particle concentration measurement in water was determined to be smaller than 25% of the reference value.

The intra-individual variability of particle size distribution and concentration on different days could only be estimated for one healthy, non-exposed subject. Figure S2 in the supplemental material indicates that the size distribution was relatively constant, with a modal size and D_{50} value of 75 ± 3 nm (CV: 4.2%) and 85 ± 5 nm (CV: 5.3%), respectively. On the contrary, particle concentration levels in EBC were more variable over the three days examined, with an average value of $(7.55 \pm 2.1) \cdot 10^7$ particles ml^{-1} (CV: 27.7%).

Table 2: Summary of NTA's performance in the determination of particle concentration in standard water solutions or EBC.

Method characteristics	Expected performance	Observed value	Conclusion
<i>Calibration function</i>			Linear
Concentration range	$1.6 \cdot 10^6 - 2.6 \cdot 10^8 \text{ \# ml}^{-1}$		
Bias for std. $1.6 \cdot 10^6 \text{ \# ml}^{-1}$ ^a	-	$496 \pm 55\%$	
Bias for std. $6.4 \cdot 10^6 \text{ \# ml}^{-1}$	120%	$121 \pm 14\%$	Verified
Bias for std. $1.6 \cdot 10^7 \text{ \# ml}^{-1}$	60%	$46 \pm 7\%$	Verified
Bias for std. $3.2 \cdot 10^7 \text{ \# ml}^{-1}$	25%	$21 \pm 4\%$	Verified
Bias for std. $6.4 \cdot 10^7 \text{ \# ml}^{-1}$	10%	$8.6 \pm 3\%$	Verified
Bias for std. $9.6 \cdot 10^7 \text{ \# ml}^{-1}$	10%	$4.4 \pm 3\%$	Verified
Bias for std. $1.3 \cdot 10^8 \text{ \# ml}^{-1}$	10%	$2.4 \pm 3\%$	Verified
Bias for std. $2.6 \cdot 10^8 \text{ \# ml}^{-1}$	10%	$-0.8 \pm 3\%$	Verified
<i>LOQ (a priori estimate)</i>			Accepted
Maximum accepted range	$(1.3 \cdot 10^7 \pm 0.78) \cdot 10^7 \text{ \# ml}^{-1}$ $= 60\% \cdot 1.3 \cdot 10^7 \text{ \# ml}^{-1}$		
Upper accepted value	$2.1 \cdot 10^7 \text{ \# ml}^{-1}$	$1.8 \cdot 10^7 \text{ \# ml}^{-1}$	Verified
Lower accepted value	$5.2 \cdot 10^6 \text{ \# ml}^{-1}$	$7.0 \cdot 10^6 \text{ \# ml}^{-1}$	Verified
LOD (1/3 LOQ) ^b		$4.3 \cdot 10^6 \text{ \# ml}^{-1}$	
<i>Recovery</i>			
EBC not spiked		$(2.94 \pm 0.62) \cdot 10^7 \text{ \# ml}^{-1}$	
EBC spiked level 1 ^c	$4.1 \cdot 10^7 \text{ \# ml}^{-1}$	$(4.26 \pm 0.44) \cdot 10^7 \text{ \# ml}^{-1}$	
EBC spiked level 2 ^d	$5.3 \cdot 10^7 \text{ \# ml}^{-1}$	$(6.20 \pm 0.62) \cdot 10^7 \text{ \# ml}^{-1}$	
Recovery EBC level 1	80%–120%	$100 \pm 18\%$	Verified
Recovery EBC level 2	80%–120%	$117 \pm 20\%$	Verified
<i>Repeatability (CV^e)</i>			
EBC not spiked	25%	21.0%	Verified
EBC spiked level 1	20%	10.3%	Verified
EBC spiked level 2	10%	9.9%	Verified
<i>Accuracy</i>			
<i>Standard solution (Q-Nano)</i>			
Reference value	$3.42 \cdot 10^8 \text{ \# ml}^{-1}$	$(3.71 \pm 0.27) \cdot 10^8 \text{ \# ml}^{-1}$	
CV		7.3%	
Maximum accepted range	$8.55 \cdot 10^7 \text{ \# ml}^{-1} = 25\% \cdot 3.42 \cdot 10^8 \text{ \# ml}^{-1}$		
Upper accepted value	$4.28 \cdot 10^8 \text{ \# ml}^{-1}$	$4.25 \cdot 10^8 \text{ \# ml}^{-1}$	Verified
Lower accepted value	$2.57 \cdot 10^8 \text{ \# ml}^{-1}$	$3.17 \cdot 10^8 \text{ \# ml}^{-1}$	Verified

^a: \# ml^{-1} : particles ml^{-1}

^b: LOD: limit of detection; LOQ: limit of quantification

^c: Level 1: $1.2 \cdot 10^7 \text{ \# ml}^{-1}$

^d: Level 2: $2.4 \cdot 10^7 \text{ \# ml}^{-1}$

^e: CV: coefficient of variation

Field study

Population and exposure assessment

The study population's general characteristics and the exposure assessment results are presented in Table 3. We quantified silica dust levels in 52 and 32 respirable dust samples from crystal quartz workers and soapstone workers, respectively. Whereas the respirable dust concentration was the highest for the soapstone workers, the crystal quartz group was more exposed to silica dust, as expected. We found a statistically significant correlation between FEV₁ (% predicted) and silica dust concentrations (Pearson correlation coefficient: - 0.31; p=0.007) but not with respirable dust concentrations (p=0.9).

Table 3: Study population's general characteristics and exposure assessment results. Data are presented as mean ± standard deviation.

	Controls (n=11)	Soapstone workers (n=55)	Crystal stone workers (n=12)	p*
Age (years)	40 ± 6	48 ± 13	33 ± 7	< 0.001
Sexe (M/F) ^a	9/2	36/19	12/0	0.04
Tobacco status (S/ES/NS) ^b	1/1/9	10/19/26	0/2/10	0.07
Tobacco consumption (pack-years)	22 ± 30	11 ± 15	10 ± 1	0.6
FEV ₁ (L) ^c	3.78 ± 0.85	3.11 ± 0.90	3.29 ± 0.67	0.08
FEV ₁ (% predicted) ^c	97 ± 16	93 ± 19	78 ± 14	0.03
Respirable dust concentration (mg.m ⁻³)	-	1.61 ± 1.19	0.96 ± 0.76	0.003
Silica dust concentration (mg.m ⁻³) ^d	-	0.1 ± 0.04	0.46 ± 0.41	0.03

^a : M: male; F: female

^b: S: smoker ; ES: ex-smoker ; NS: non smoker

^c: FEV₁: Forced expiratory volume in one second

^d: average of sample concentrations in which the silica was detectable

*: p-values of one-way ANOVA or Fisher exact test

EBC analysis for particles

After collection, EBC samples were transported at -20°C and stored at -80°C in the laboratory. RTubes[®] were used without treatment as they are cleaned to factory standards (alcohol followed by deionized water followed by forced air drying) before being packaged in plastic bags. We tested that this cleaning treatment ensured sampling tubes free of exterior particulate contamination for the NTA.

Flickering was often observed on the EBC sample videos for crystal quartz workers (see Videos 1, 2 and 3, Supplemental material). Some very bright particles were present in addition to other less intensely reflective particles. This added background-light intensity made tracking particles which scattered light more weakly more difficult for the NTA software. Selected examples of number size and cumulative size distributions in EBC are presented in Figure 1. The average size characteristics for particles detected in the EBC of the three different groups are shown in Table S1 (Supplemental material) in terms of mean, mode, D_{10} , D_{50} and D_{90} .

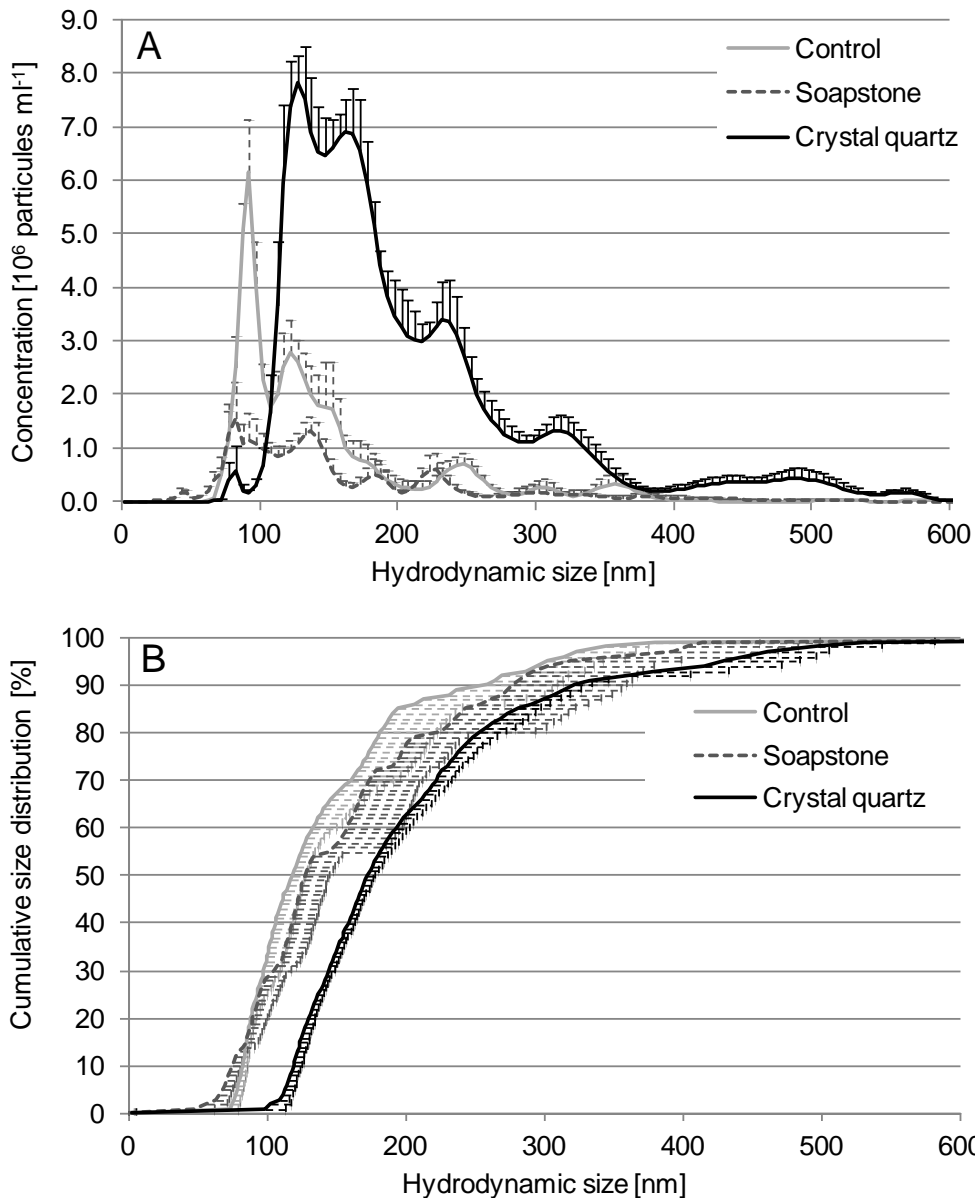


Figure 1: Typical size distribution (A) and corresponding cumulative curves (B) of particles in EBC collected from one control, one exposed soapstone worker and one exposed crystal quartz worker. Error bars correspond to the standard deviation of five separate videos from the same EBC sample.

The particle size distributions from all the biological samples were very polydisperse, with a standard deviation ranging from 31–119 nm. For the control EBC, 80% of the particles ranged from 90–250 nm, similar to EBC from workers exposed to soapstone (75–240 nm). For EBC collected from crystal quartz workers, this range was skewed towards larger values (110–

290 nm; see Table S1, Supplemental material). All the particle size variables (see Table S1, Supplemental material) were significantly higher for crystal quartz than for soapstone and the controls ($p < 0.01$ post hoc t-test with Bonferroni corrections). Also, a statistically different D_{10} size was observed between the control group and the soapstone group ($p < 0.01$ post hoc t-test with Bonferroni corrections). Inter-individual particle size variability, as characterized by the CV and calculated by taking the ratio of the standard deviation to the average value for each group of the different size distribution parameters, ranged between 7%–27%. It is of note that the lowest inter-individual variabilities were observed for workers in the crystal quartz group (always smaller than 10%).

There was a statistically significant difference between the total particle concentration in the EBC from workers processing crystal quartz ($20.1 \pm 4.6 \cdot 10^7$ particles ml^{-1}) and the concentrations in the other two groups (control: $2.8 \pm 1.6 \cdot 10^7$ particles ml^{-1} ; soapstone: $4.2 \pm 1.9 \cdot 10^7$ particles ml^{-1} ; $p < 0.01$ post hoc t-test with Bonferroni corrections; see Figure S3, Supplemental material). The inter-individual particle concentration variabilities in each group were rather high, reaching 58%, 45%, and 24% for the control, soapstone, and crystal quartz groups, respectively. Again, the lowest inter-individual variability was observed among crystal quartz workers. We also evaluated particle concentrations in five different size ranges (0–102 nm; 102–202 nm; 203–302 nm; 303–502 nm; > 503 nm) as illustrated in Figure 2. A significant increase in the concentration of particles with sizes above 102 nm was observed in the EBC collected from the crystal quartz workers. On the contrary, controls and worker exposed to soapstone presented very similar size distributions.

NTA cannot determine the precise nature of the particles detected in EBC. In order to get additional information about these particles, EBC samples were air dried on carbon-coated grids and observed using scanning electron microscopy with energy dispersive X-ray spectroscopy (SEM-EDX). Some examples of the particles detected are presented in Figure S4, with their corresponding EDX spectra. Two groups of particles were identifiable in the EBC samples considered: one group was composed mainly of sodium (Na), potassium (K), chlorine (Cl), and sulfur (S); the second also contained alkaline earth metals (Ca, Mg), metalloids (Al, Si), and metal elements (Fe, Ti).

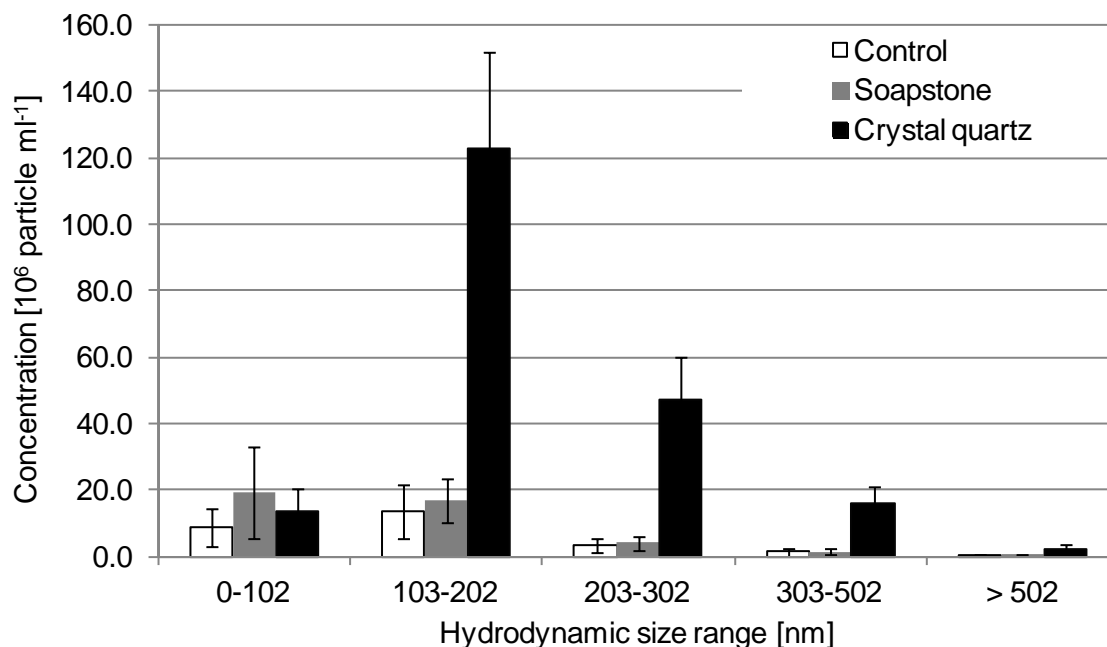


Figure 2: Average particle concentrations in EBC as a function of five different size fractions for the three different groups. Error bars correspond to the standard deviation of all the samples in each group (control: n = 11; soapstone: n = 55; crystal stone: n = 12).

Discussion

To the best of our knowledge, this study is the first to qualify and quantify the particles in the exhaled breath condensate (EBC) of workers exposed to quartz or steatite dust, using a validated nanoparticle tracking analysis (NTA) method. Our results showed that the NTA technique performed well when characterizing the size distributions and concentrations of particles in EBC. All the particle size variables were significantly higher for crystal quartz than for soapstone and controls. Our study also showed that the total particle concentrations in the EBC of workers processing crystal quartz were significantly higher than those of the two other groups (soapstone and controls).

The lowest particle sizes detected in all the EBCs were in the range of 45–55 nm. This value is in accord with data in the literature which reported NTA's detection limit of 30 nm for proteins [16]. This value may vary, however, as NTA's sensitivity depends on the difference between the refractive indices of the nanoparticles and their carrying medium [23]. When EBC was spiked with low levels of concentrated polystyrene latex (PSL) beads, NTA showed very good

repeatability (less than 8% variability) for the D_{50} size—comparable with other studies [17]. In addition, we measured a mode particle size of 104 ± 6 nm, which corresponded quite well to the beads' nominal size of 100 nm. This result suggested that the presence of proteins in EBC [24], which are potentially able to adsorb on the polystyrene latex surface, do not influence the hydrodynamic size of these PSL beads. NTA has been reported as able to detect hydrodynamic size increases of about 10 nm when gold nanoparticles are put in contact with fetal calf serum. This size increase is attributed to the formation of a protein corona [25]. Thus, in the present study, size measurements were probably not affected by artifacts (agglomeration). The fact that EBC can be analyzed directly, without any preparation, makes NTA an interesting technique, as the dilution of particle suspensions can affect their size distributions [23].

The latest developments in NTA software (version 3.1 was used in this study) provide increased confidence in the concentration data which can be obtained using this technique. Repeatability, as evaluated with a coefficient of variation (CV) of 10%, has been reported for concentration measurements in tests with the upgraded version of NTA [26]. This compares very well to the CV obtained in the present study (9.9%–21%, Table 2). The greater variability observed in concentrations in non-spiked EBC (CV = 21%, Table 2), in comparison to size measurements (D_{50} : CV = 12%, Table 1), might be due to the difficulties in detecting and counting small particles in the presence of larger ones. Filipe *et al.* [16] described the analysis of a standard PSL bead mixture (100 nm, 400 nm, 1000 nm; ratio 1:1:267); the concentrations of 100 nm and 400 nm PSL beads detected decreased by 70% and 20%, respectively, in comparison to a mixture analyzed without large particles. This suggests that polydisperse suspensions with large light diffusing particles might hinder NTA's detection of smaller particles. One frequently mentioned difficulty holding back the use of EBC in clinical settings is the lack of methodological standardization, as this leads to large variability in the published data [27]. The fact that NTA measurement is highly automated, with only a small number of software variables requiring definition by the user, implies reduced inter-laboratory variability [17].

We were able to detect particles in low concentrations in all the EBC samples, but generally above the determined LOQ of $1.3 \cdot 10^7$ particles ml^{-1} . Only 2.5% of all the EBC samples (and only control samples) showed concentration values smaller than this LOQ. The very different size distribution of particles in the EBC of craftsmen working with crystal quartz, in comparison to soapstone workers and controls (Figure 1), suggests that exposure to aerosols generated from quartz increases the particle concentration measured in EBC. Nevertheless, as presented in Table 3 and Figure S3, the particle concentration in EBC does not appear to be related to the

respirable concentration as the greatest exposure observed for soapstone workers corresponded to a very low particle concentration in EBC, similar to the controls. On the contrary, the content of silica in the respirable fraction followed the same trend as the particle concentration observed in the EBC (Table 3 and Figure S3). The silica content in the respirable fraction of crystal quartz workers was five times larger than that of soapstone workers, and this translated into a similar increase in the particle concentrations observed in EBC of the crystal quartz worker group. Furthermore, this influence was mostly observed for particle sizes larger than 100 nm (Figure 2). These results may suggest that the number of quartz particles is greater in the EBC of crystal quartz workers because they remain in the alveolar compartment longer than amorphous particles such as those in soapstone dust. Indeed, EBC mainly originates deep in the lungs [28] and most fine particles (i.e. less than 2.5 microns) are typically deposited in the lung acini [29]. In addition, Arts *et al.* [30] showed that the pulmonary clearance time of quartz particles in rats was longer than that of amorphous particles. Our results may thus be explained by a lack of lung clearance of quartz particles, which favors their biopersistence in the airway lining fluid. Due to technical difficulties, it was impossible to assess the granulometry of the particles to which the workers were exposed. Nevertheless, the particulate content in the EBC of crystal quartz workers was significantly different from that of soapstone workers or controls. Thus, the EBC matrix appears to be a reflection of the lungs' particulate content. The FEV₁ values of the crystal quartz group were lower than the other groups taking into account age and smoking consumption. These findings are consistent with Ulvestad *et al.* [31] who showed that the decline in FEV₁ was greater (50 to 63 mL per year) in tunnel workers exposed to lower alpha-quartz concentrations (between 0.019 and 0.044 mg.m⁻³) compared to control subjects (25 mL per year). Therefore, the low values of FEV₁ observed in crystal quartz workers can be explained by exposure to silica dust.

The possible influence of active smoking on the particle concentration in EBC could only be evaluated for the soapstone workers' group, as it contained the largest number of smoking volunteers (10 out of 55). No statistically significant contribution of smoking to the particle concentrations in EBC was observed (post hoc t-test with Bonferroni corrections, data not shown). Although this result is based on a relatively small amount of data, it is consistent with previous literature [12, 14] which failed to find any association between the number of particles in EBC and smoking status.

The fact that the EBC samples of all three groups revealed a similar size distribution in the range from 0–102 nm suggests either that the processing of soapstone and crystal quartz only

emit a small fraction of nanoparticles (with sizes smaller than 100 nm) or that it is difficult to detect small particles when their suspension is of a polydisperse nature. Another explanation could be that when samples are not flash frozen, the nanoparticles in EBC undergo a faster dissolution rate, as reported for tungsten particles from inert gas welding [32]. Such similar concentrations of particles smaller than 100 nm could also point to their endogenous origin. The NTA technique has been shown to detect particles of biological origin, such as microvesicles or exosomes [33], with sizes corresponding to the size range observed for control EBCs. Additionally, data from Almstrand *et al.* [34] suggest that the exhaled particles could correspond to lipidic bilayered vesicles of endogenous origin.

The precise nature of the particles measured in EBC cannot be determined using NTA, but scanning electron microscopy (SEM) techniques allowed us to make a morphological and qualitative chemical analysis. The particles observed using this technique were rather large, with irregular shapes and approximate sizes between 0.5 and > 10 μm (see Figure S4, Supplemental material). Energy dispersive X-ray spectroscopy (EDX) analysis indicated the recurrent presence of sodium (Na), potassium (K), chlorine (Cl), and sulfur (S) elements, together with the less frequent presence of alkaline earth metals (Ca, Mg), metalloids (Al, Si), and transition metals (Fe, Ti). The objects containing Na, K, Cl, and S in addition to carbon and oxygen are thought to originate either from the airway lining fluid itself [14, 35], after recrystallization during the drying process on the grid, or from some external source [10, 34]. The other elements detected are potentially constituents of the soapstone rocks and crystal quartz used in this region [36]. By combining different techniques (SEM and NTA), it was possible to confirm that EBC contains particles originating from the materials processed by the workers. Nevertheless, it was impossible to disentangle the endogenous origin (microvesicles or cellular debris) of the particles detected in the different EBC samples from exogenous ones (ambient particles for controls and/or workplace-generated particles of soapstone and crystal quartz).

Conclusions

The ability to make a non-invasive determination of the doses of particles deposited in subjects' lungs would greatly help our understanding of their subsequent biological effects. The NTA technique shows promise in this domain, as the present study describes it to be a sensitive and reliable method for the characterization of particle size distributions and concentrations in EBC.

Applying the NTA technique to EBC samples collected from controls and workers exposed to soapstone or crystal quartz dust revealed that only those volunteers exposed to crystal quartz showed statistically higher concentrations of particles in their EBC. This observation suggests that exposure to crystal quartz particles influences particle concentrations measured in EBC. This influence is mainly apparent for particle sizes larger than 100 nm. NTA alone can provide important information about the size distributions and concentration levels of particles in EBC, however, it must be combined with other techniques (SEM/TEM, or single particle ICP-MS for metallic particles) in order to determine the precise nature of those particles. Many issues will have to be resolved before such a technique could be proposed for determining the dose deposited in the lungs as a proxy for exposure. The relationship between the characteristics of inhaled particles (size distribution and number) and those of the particles measured in EBC is of prime importance. Further studies using well-controlled experimental situations, e.g. using monodispersed particles or different breathing scenarios, will also be needed to assess the contributions of endogenous and exogenous particles to the total numbers and size distributions of the particles measured using NTA.

Acknowledgments

The authors would like to thank Dr. N. Concha-Lozano for his helpful discussions about the SEM data. This work was supported by “Action en Région de Coopération Universitaire et Scientifique” (ARCUS) (a partnership between France and Brazil) and the “Fundação de Amparo a Pesquisa do Estado de Minas Gerais” (FAPEMIG).

Conflict of interest

The authors declare no conflicts of interests.

References

- [1] Donaldson K, Schinwald A, Murphy F, Cho W-S, Duffin R, Lang T, Poland C 2013 The Biologically Effective Dose in Inhalation Nanotoxicology *Acc. Chem. Res.* **46** 723-732.
- [2] Braakhuis HM, Park MVDZ, Gosens I, De Jong WH, Cassee FR 2014 Physicochemical characteristics of nanomaterials that affect pulmonary inflammation *Part. Fibre Toxicol.* **11** 18.

- [3] Oberdorster G, Oberdorster E, Oberdorster J 2005 Nanotoxicology: An emerging discipline evolving from studies of ultrafine particles *Environ. Health Perspect.* **113** 823-839.
- [4] Schmid O, Moller W, Semmler-Behnke M, Ferron GA, Karg E, Lipka J, Schulz H, Kreyling WG, Stoeger T 2009 Dosimetry and toxicology of inhaled ultrafine particles *Biomarkers* **14** 67-73.
- [5] Kim CS 2009 Deposition of aerosol particles in human lungs: in vivo measurement and modelling *Biomarkers* **14** 54-58.
- [6] Peters A, Wichmann HE, Tuch T, Heinrich J, Heyder J 1997 Respiratory effects are associated with the number of ultrafine particles *Am. J. Respir. Crit. Care Med.* **155** 1376-1383.
- [7] Hunt J 2007 Exhaled breath condensate: An overview *Immunol. Allergy Clin. North Am.* **27** 587-596.
- [8] Koutsokera A, Loukides S, Gourgoulianis KI, Kostikas K 2008 Biomarkers in the exhaled breath condensate of healthy adults: Mapping the path towards reference values *Curr. Med. Chem.* **15** 620-630.
- [9] Falgayrac G, Cherot-Kornobis N, de Broucker V, Hulo S, Edme J-L, Sobaszek A, Penel G 2011 Noninvasive molecular identification of particulate matter in lungs by Raman microspectrometry *J. Raman Spectrosc.* **42** 1484-1487.
- [10] Pinheiro T, Alexandra Barreiros M, Alves LC, Felix PM, Franco C, Sousa J, Almeida SM 2011 Particulate matter in exhaled breath condensate: A promising indicator of environmental conditions *Nucl. Instrum. Met. B* **269** 2404-2408.
- [11] Felix PM, Franco C, Barreiros MA, Batista B, Bernardes S, Garcia SM, Almeida AB, Almeida SM, Wolterbeek HT, Pinheiro T 2013 Biomarkers of Exposure to Metal Dust in Exhaled Breath Condensate: Methodology Optimization *Arch. Environ. Occup. Health* **68** 72-79.
- [12] Sauvain J-J, Hohl MSS, Wild P, Pralong JA, Riediker M 2014 Exhaled Breath Condensate as a Matrix for Combustion-Based Nanoparticle Exposure and Health Effect Evaluation *J. Aerosol Med. Pulm. Drug Delivery* **27** 449-458.
- [13] Benor S, Alcalay Y, Domany KA, Gut G, Soferman R, Kivity S, Fireman E 2015 Ultrafine particle content in exhaled breath condensate in airways of asthmatic children *J. Breath Res.* **9** 026001.
- [14] Marie-Desvergne C, Dubosson M, Touri L, Zimmermann E, Gaude-Môme M, Leclerc L, Durand C, Klerlein M, Molinari N, Vachier I et al 2016 Assessment of nanoparticles and metal exposure of airport workers using exhaled breath condensate *J. Breath Res.* **10** 036006.
- [15] Pelclova D, Barosova H, Kukutschova J, Zdimal V, Navratil T, Fenclova Z, Vlckova S, Schwarz J, Zikova N, Kacer P et al 2015 Raman microspectroscopy of exhaled breath condensate and urine in workers exposed to fine and nano TiO₂ particles: a cross-sectional study *J. Breath Res.* **9** 036008.

- [16] Filipe V, Hawe A, Jiskoot W 2010 Critical Evaluation of Nanoparticle Tracking Analysis (NTA) by NanoSight for the Measurement of Nanoparticles and Protein Aggregates *Pharm. Res.* **27** 796-810.
- [17] Hole P, Sillence K, Hannell C, Maguire CM, Roesslein M, Suarez G, Capracotta S, Magdolenova Z, Horev-Azaria L, Dybowska A *et al* 2013 Interlaboratory comparison of size measurements on nanoparticles using nanoparticle tracking analysis (NTA) *J. Nanopart. Res.* **15** 2101.
- [18] AFNOR 2009 Water quality- Protocol for the initial method performance assessment in a laboratory NF T 90-210 La Plaine Saint-Denis Cedex AFNOR.
- [19] FUNDACENTRO 2006 Norma de Higiene ocupacional-Coleta de material particulado sólido suspenso no ar de ambientes de trabalho In., vol. NH08: Fundação Jorge Duprat Figueiredo de Segurança e Medicina do Trabalho.
- [20] Santos AMA 1989 Determinação quantitativa de sílica livre cristalizada por difração de Raios-X *Rev. Bras. Saúde Ocup.* **17** 55-59.
- [21] Horvath I, Hunt J, Barnes PJ 2005 Exhaled breath condensate: methodological recommendations and unresolved questions *Eur. Respir. J.* **26** 523-548.
- [22] Pereira CA, Sato T, Rodrigues SC 2007 New reference values for forced spirometry in white adults in Brazil *J Bras. Pneumol.* **33** 397-406.
- [23] Gallego-Urrea JA, Tuoriniemi J, Pallander T, Hasselov M 2009 Measurements of nanoparticle number concentrations and size distributions in contrasting aquatic environments using nanoparticle tracking analysis *Environ. Chem.* **7** 67-81.
- [24] Kuban P, Foret F 2013 Exhaled breath condensate: Determination of non-volatile compounds and their potential for clinical diagnosis and monitoring. A review *Anal. Chim. Acta* **805** 1-18.
- [25] Montes-Burgos I, Walczyk D, Hole P, Smith J, Lynch I, Dawson K 2010 Characterisation of nanoparticle size and state prior to nanotoxicological studies *J. Nanopart. Res.* **12** 47-53.
- [26] Technical note: NanoSight NTA Concentration Measurement Upgrade [<http://www.malvern.com/fr/pdf/secure/TN150515NTAConcentrationUpgrade.pdf>]
- [27] Bredberg A, Gobom J, Almstrand A-C, Larsson P, Blennow K, Olin A-C, Mirgorodskaya E 2012 Exhaled Endogenous Particles Contain Lung Proteins *Clin. Chem.* **58** 431-440.
- [28] Johnson GR, Morawska L 2009 The Mechanism of Breath Aerosol Formation *J. Aerosol Med. Pulm. Drug Delivery* **22** 229-237.
- [29] International Commission on Radiological Protection: Human Respiratory Tract Model for Radiological Protection, vol. 66. Oxford: Elsevier Science Ltd.; 1994.
- [30] Arts JHE, Muijser H, Duistermaat E, Junker K, Kuper CF 2007 Five-day inhalation toxicity study of three types of synthetic amorphous silicas in Wistar rats and post-exposure evaluations for up to 3 months *Food Chem. Toxicol.* **45** 1856-1867.

- [31] Ulvestad G, Bakke B, Eduard W, Kongerud J, Lund MB 2001 Cumulative exposure to dust causes accelerated decline in lung function in tunnel workers *Occup. Environ. Med.* **58** 663-669.
- [32] Gschwind S, Graczyk H, Gunther D, Riediker M 2016 A method for the preservation and determination of welding fume nanoparticles in exhaled breath condensate *Environ. Sci. Nano* **3** 357-364.
- [33] Lawson C, Vicencio JM, Yellon DM, Davidson SM 2016 Microvesicles and exosomes: new players in metabolic and cardiovascular disease *J. Endocrinol.* **228** R57-R71.
- [34] Almstrand AC, Ljungstrom E, Lausmaa J, Bake B, Sjoval P, Olin AC 2009 Airway monitoring by collection and mass spectrometric analysis of exhaled particles *Anal. Chem.* **81** 662-668.
- [35] Greenwald R, Fitzpatrick AM, Gaston B, Marozkina NV, Erzurum S, Teague WG 2010 Breath Formate Is a Marker of Airway S-Nitrosothiol Depletion in Severe Asthma *PLoS ONE* **5** e11919.
- [36] Rodrigues MLM, Lima RMF 2012 Cleaner production of soapstone in the Ouro Preto region of Brazil: a case study *J. Clean. Prod.* **32** 149-156.